

A VERY BRIGHT, HIGHLY MAGNIFIED LYMAN BREAK GALAXY AT $z = 3.07$

IAN SMAIL,¹ A. M. SWINBANK,¹ J. RICHARD,² H. EBELING,³ J.-P. KNEIB,⁴ A. C. EDGE,¹ D. STARK,²
R. S. ELLIS,² S. DYE,⁵ G. P. SMITH,⁶ AND C. MULLIS⁷

Received 2006 August 4; accepted 2006 November 16; published 2006 December 20

ABSTRACT

Using *Hubble Space Telescope* imaging and Keck spectroscopy, we report the discovery of a very bright, highly magnified (~ 30 times) Lyman break galaxy (LBG) at $z = 3.07$ in the field of the massive $z = 0.33$ cluster MACS J2135.2–0102. The system comprises two high surface brightness arcs with a maximum extent of $3''$, bracketing a central object that we identify as a massive early-type galaxy at $z = 0.73$. We construct a lens model that reproduces the main features of the system using a combination of a galaxy-scale lens and the foreground cluster. We show that the morphological, spectral, and photometric properties of the arcs are consistent with them arising from the lensing of a single $\sim L^*$ LBG. The most important feature of this system is that the lensing magnification results in an apparent magnitude of $r = 20.3$, making this one of the brightest LBGs known. Such a high magnification provides the opportunity of obtaining very high signal-to-noise ratio (and potentially spatially resolved) spectroscopy of a high-redshift galaxy to study its physical properties. We present initial imaging and spectroscopy demonstrating the basic properties of the system and discuss the opportunities for future observations.

Subject headings: cosmology: observations — galaxies: evolution — galaxies: formation — galaxies: individual (LBG J213512.73–010143)

Online material: color figures

1. INTRODUCTION

Some of the most compelling science drivers from the extragalactic research field for the construction of extremely large telescopes (ELTs) involve investigating the internal dynamics of the gas and stars, and the chemical abundances of these components, in faint high-redshift galaxies (Hook 2005). This requires a combination of high spatial resolution and high signal-to-noise ratio (S/N) spectroscopy that only the largest telescope apertures can provide. These observations will yield insights into the physical properties of star formation in the early universe. Yet some of these scientific questions can be tackled with the current generation of 10 m class telescopes, when aided by the natural magnification provided by a gravitational lens. Such lens-aided studies are already providing some of our most sensitive views of the distant universe, with lensing surveys for faint sources out to the highest redshifts and across a range of wave bands (e.g., Ellis et al. 2001; Smail et al. 2002; Santos et al. 2004; Kneib et al. 2004a, 2004b).

In terms of our understanding of the internal properties of high-redshift galaxies, the studies of the gravitationally lensed Lyman break galaxy (LBG) cB58 by Pettini et al. (2000, 2002) have demonstrated that high S/N spectra of typical LBGs can be obtained with 10 m telescopes, if they are highly magnified as a result of being serendipitously positioned behind a suitable foreground gravitational lens; cB58 has an apparent magnitude of $r = 20.4$ and represents a $\sim 30 \pm 10$ times magnified image of an L^* LBG at $z = 2.72$. The studies of this object have yielded a wealth of information on the metallicity and energetics of the interstellar medium (ISM) in a young star-forming galaxy (Pettini et al. 2002). The only drawback with these

studies is the difficulty in drawing wide-ranging conclusions from a single object and hence the urgent need to find other examples of similarly highly magnified galaxies. To this end, several deep imaging surveys of clusters have been undertaken to search for highly magnified LBGs using *U*- and *B*-band dropout selection (e.g., Smail et al. 1998; Stern et al. 2004). The difficulty for these surveys is the presence of large numbers of red galaxies in the clusters, whose spectral properties are sufficiently similar to the target population to be a significant source of contamination, and so far they have not yet yielded any highly magnified, high-redshift galaxies as bright as cB58. Similarly, attempts to use the wide area coverage of the Sloan Digital Sky Survey (SDSS) to identify rare, intrinsically bright, or highly magnified LBGs (Bentz et al. 2004) have until recently only uncovered an unusual class of active galactic nuclei with weak rest-frame UV emission lines (Ivion et al. 2005). However, Allam et al. (2007) have just announced the discovery of a bright lensed LBG using data from SDSS.

In this Letter we present the discovery of a $z = 3.07$ galaxy, LBG J213512.73–010143, which appears as two highly magnified arcs with an apparent magnitude of $r = 20.3$, making it slightly brighter than cB58. We assume a cosmology with $\Omega_m = 0.27$, $\Omega_\Lambda = 0.73$, and $H_0 = 71 \text{ km s}^{-1} \text{ Mpc}^{-1}$, giving angular scales of 4.7, 7.3, and 7.8 kpc arcsec⁻¹ at $z = 0.33$, 0.73, and 3.08, respectively. All quoted magnitudes are on the AB system.

2. OBSERVATIONS AND REDUCTION

2.1. *HST* Imaging

We obtained a 1.2 ks *Hubble Space Telescope* (*HST*) Advanced Camera for Surveys (ACS) F606W image of MACS J2135.2–0102 on 2006 May 8, as part of our Snapshot program (GO 10491; PI: H. Ebeling). This program targets high-luminosity X-ray clusters to identify bright lensed galaxies and constrain the cluster mass distributions. MACS J2135.2–0102 is a high-luminosity X-ray cluster at $z = 0.325$ cataloged by Ebeling et al. (2001). The ACS exposure comprised three 400 s exposures dithered with a

¹ Institute for Computational Cosmology, Durham University, Durham, UK.

² California Institute of Technology, Department of Astronomy, Pasadena, CA.

³ Institute for Astronomy, Honolulu, HI.

⁴ Laboratoire d'Astrophysique de Marseille, Marseille Cedex, France.

⁵ School of Physics and Astronomy, Cardiff, UK.

⁶ School of Physics and Astronomy, University of Birmingham, Edgbaston, Birmingham, UK.

⁷ Department of Astronomy, University of Michigan, Ann Arbor, MI.

LINE pattern and a 3" spacing. The data were reduced using *multidrizzle* version 2.7 to provide an image with 0.05" sampling and good cosmetic properties.

A visual inspection of the *HST* image by two of us (A. C. E. and A. M. S.) identified an unusual object at $21^{\text{h}}35^{\text{m}}12.730^{\text{s}}$, $-01^{\circ}01'42.9'' \pm 0.5''$ (J2000.0), lying approximately $75''$ due north of the brightest cluster galaxy ($21^{\text{h}}35^{\text{m}}12.08^{\text{s}}$, $-01^{\circ}02'58''$, J2000.0). In the *HST* ACS image, Figure 1, the object appears as two nonconcentric arcs, enclosing a central compact object and is reminiscent of a “cosmic eye.” We denote the northern and southern arcs as N and S, respectively, and the central source as G1. Interestingly, the centers of curvature of N and S do not coincide (Fig. 1). The radii of curvature are $1.0''$ for N, which is nearly perfectly circular, and $1.5''$ for S, which is more flattened. The faint, western extension of N has a radius of curvature of $1.3''$.

A search of the SDSS Data Release 4 shows that this object is well detected with a total magnitude of $r = 20.27$, consistent with the *HST* measurement of $R_{606} = 20.54 \pm 0.02$ for the light from both arcs, and $R_{606} = 21.06 \pm 0.05$, $R_{606} = 21.60 \pm 0.10$, and $R_{606} = 22.34 \pm 0.15$ for N, S, and G1 respectively. The arcs are unresolved across their width, with apparent FWHM of $\sim 0.15''$ along their whole lengths: $2.2''$ for N and $2.8''$ for S, yielding axial ratios of >15 and >19 , respectively. In contrast, G1 has a FWHM of $\sim 0.25''$ with an ellipticity of $\epsilon \sim 0.3$ at a position angle (P.A.) of 105° (i.e., aligned along the major axis of the arcs).

2.2. Keck Spectroscopy and Imaging

The morphology of this source is strongly suggestive of gravitational lensing, with G1 being the lens. In addition, the SDSS *griz* colors are blue [$(g - r) = 1.20$, $(r - i) = 0.53$, and $(i - z) = 0.29$] but with a red $(u - g) = 2.30$ color, indicating a spectral break shortward of the *g* band and hence a probable redshift of $z \sim 3$ –4. Therefore, we observed the system as a high priority with the Low Resolution Imaging Spectrograph (LRIS) on the Keck I telescope on the night of 2006 June 30 in good transparency and $\lesssim 1.0''$ seeing. The system was observed at two position angles (P.A. of 55° and 120° ; Fig. 1) to cover both arcs and G1. We employed the 600 line mm^{-1} grism in the blue arm, blazed at 4000 \AA , and the 400 line mm^{-1} grating in the red arm, blazed at 8500 \AA , giving wavelength coverage from the atmospheric cutoff out to $\sim 9000 \text{ \AA}$. The total integration at each P.A. was 3.6 ks. The spectra were reduced with standard IRAF and IDL routines to yield fluxed, wavelength-calibrated spectra. We show the individual spectra for each arc and the total combined spectrum in Figure 2. A spectrum was also extracted for G1.

In addition, we obtained a 2.4 ks exposure with Near Infrared Spectrometer (NIRSPEC) on Keck II on the night of 2006 July 24. This observation, taken at P.A. of 55° , covered the entire *K*-band window and detected continuum and a series of narrow emission lines from the eastern component of S (see Fig. 2, *inset*). Finally, we obtained a *K'*-band image of the system with the NIRC near-infrared imager on Keck I on the night of 2006 July 4. The total exposure time was 1.14 ks in $0.5''$ seeing. The image detects and resolves both arcs and the central galaxy, G1.

3. ANALYSIS AND DISCUSSION

3.1. Source Properties

The LRIS spectra (Fig. 2) show that the two arcs have blue continua with a series of strong absorption features and spectral

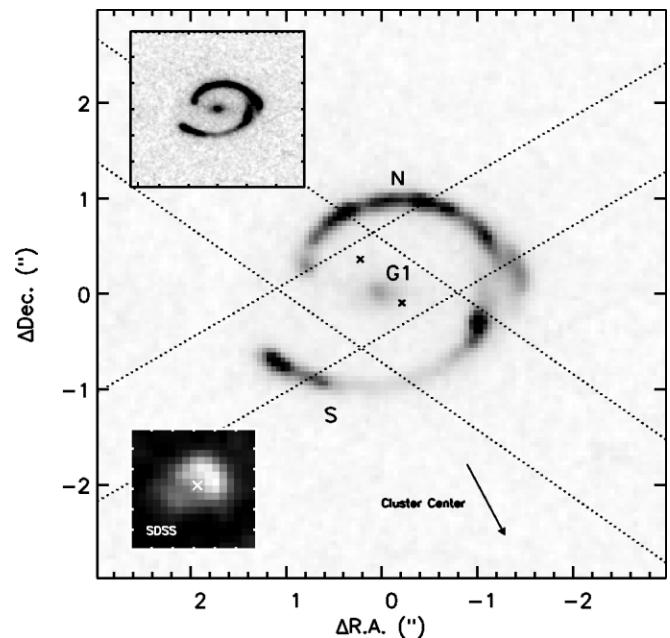


FIG. 1.—*HST* ACS F606W image of LBG J213512.73–010143 showing the twin arcs (labeled as north, N, and south, S) around a compact source, G1. Arc N has several bright knots with a symmetric appearance, along with a low surface brightness extension to the west that has a different radius of curvature. Arc S has a bright knot at each end, connected by low surface brightness emission. The two arcs are not concentric, and we mark their centers of curvature with crosses. The pairs of dotted lines indicate the alignment of the spectroscopic slits in our Keck LRIS observations. The inset to the upper left displays the same field at a higher contrast, while the inset at the lower left shows a true color SDSS *griz* image of the source; we indicate the direction to the cluster center. [See the electronic edition of the *Journal* for a color version of this figure.]

breaks that unambiguously identify the redshift at $z \sim 3.074$. The absorption features in the spectra are similar to those in the subset of the LBG population that exhibit $\text{Ly}\alpha$ in absorption (Shapley et al. 2003). In particular, we see strong absorption from species in the ISM of the galaxy, as well as broad, blueshifted absorption in the C IV $\lambda 1550$ and O I $\lambda 1302$ lines, both of which are observed in typical LBGs. One difference is that the $\text{Ly}\alpha$ absorption in the arcs is stronger than in typical LBGs and indicates a significant H I column density of $\log N(\text{H I}) \sim 21.7$ (~ 7 times higher than cB58; Pettini et al. 2000). We qualitatively compare the spectrum with the predictions from the Starburst99 model (Leitherer et al. 1999, 2001) and the *International Ultraviolet Explorer* spectra of O/B stars in de Mello et al. (2000). The strength of the C IV $\lambda 1550$ absorption, the lack of an associated red emission wing, and the relative weakness of the Si IV $\lambda 1400$ absorption suggest that the luminosity-weighted stellar population in the arcs is dominated by early B-type supergiants, indicating either a ~ 10 Myr old burst of star formation or ongoing activity over a similar or slightly longer period, but with a stellar initial mass function (IMF) deficient in O-type stars.

Analysis of the spectra for the individual subcomponents of the arcs shows no evidence for internal velocity offsets within either N and S, as expected if they are both multiply imaged. We derive redshifts, from fits to individual photospheric absorption lines (O IV $\lambda 1343.4$, Si III $\lambda 1417.2$, C III $\lambda 1427.8$, and S V $\lambda 1501.8$), for S of $z = 3.0747 \pm 0.0005$ and for N of $z = 3.0744 \pm 0.0003$ (all errors are bootstrap estimates). We caution that these features are individually weak, but they suggest that there is no significant velocity offset between the two arcs ($\lesssim 50 \text{ km s}^{-1}$). However, a comparison of the spectra of the two arcs does show some marked differences: the profiles

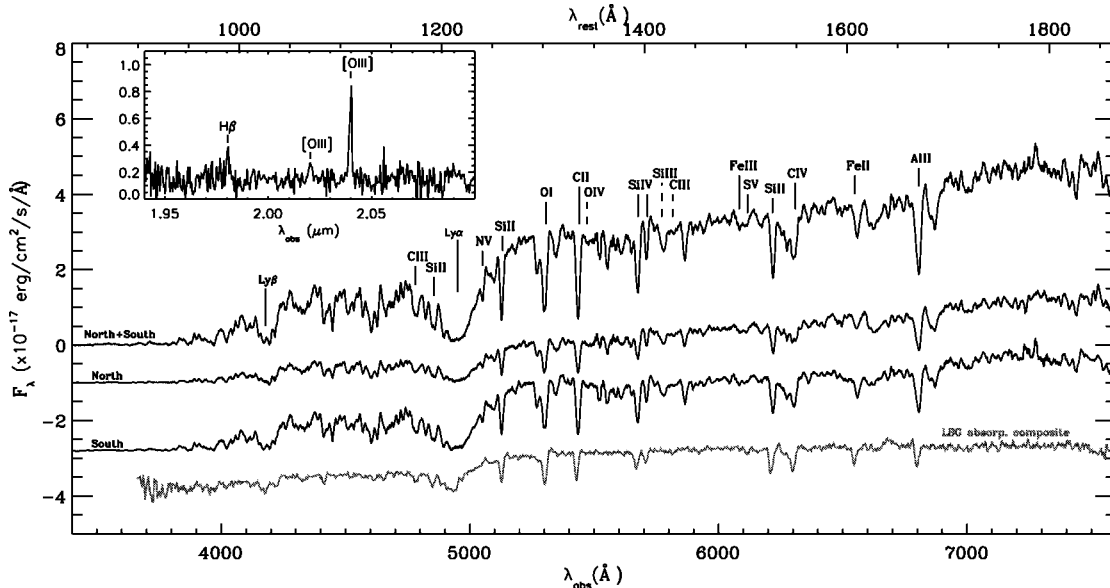


FIG. 2.—Combined Keck LRIS spectrum of the two arcs (*top*) as well as the spectra for the individual arcs, N and S (*center*). We mark the positions of the absorption features we identify in the spectra, both the strong lines arising from the ISM in the galaxy and the weaker photospheric features (*dotted lines*). The top axis gives the rest-frame wavelength scale at the systemic redshift of the source. For comparison, we show the composite spectrum of LBGs with Ly α absorption from Shapley et al. (2003); note the broad similarity in the main spectral features—apart from the stronger damping wings of the Ly α line in the lensed LBG. We also show in the inset the NIRSPEC spectrum of the eastern component of S, identifying the H β and [O III] $\lambda\lambda 4959, 5007$ lines, which yield a systemic redshift for the source of $z = 3.0743$. The flux scale of the inset is the same as the main figure. [See the electronic edition of the *Journal* for a color version of this figure.]

of the Ly α , Ly β , and the stronger ISM lines differ between N and S, and the continuum appears redder in S, indicating that N and S are images of different sources, either two galaxies, or more likely two regions within a single galaxy (consistent with the lens reconstruction).

We also measure the redshifts of the strong ISM lines in the two arcs obtaining $z = 3.0727 \pm 0.0004$ and 3.0726 ± 0.0003 for single Gaussian fits to the lines in S and N respectively, using Si II $\lambda 1260.4$, O I $\lambda 1302.2$ C II $\lambda 1334.5$, Si IV $\lambda 1402.8$, Si II $\lambda 1526.7$, and Al II $\lambda 1670.8$. Looking at the stronger ISM lines in the composite spectrum in more detail shows that they comprise at least three components: a weak one at $z = 3.0666 \pm 0.0007$ and two stronger ones at $z = 3.0715 \pm 0.0010$ and 3.0752 ± 0.008 . The reddest component has a redshift consistent with the photospheric and nebular emission-line estimates (see below), suggesting it arises in gas at the systemic redshift of the system. For the bluer ISM lines, we derive blueshifts of $-200 \pm 70 \text{ km s}^{-1}$ for the stronger line and $-570 \pm 60 \text{ km s}^{-1}$ for the weaker. These are consistent with outflows of material from the galaxy in the form of a wind, and the velocities are comparable to those seen in typical LBGs (C. C. Steidel et al. 2007, in preparation). Turning to the continuum emission we measure a rest-frame UV spectral slope for the composite spectrum between 1200 and 2000 Å of $\beta = -1.6 \pm 0.1$, which implies $A_{1600} \sim 1.7$ or $E(B - V) \sim 0.4$ (Calzetti et al. 2000). We also see a sharp decline in flux as we move blueward of Ly β , with little detectable emission shortward of 930 Å in the rest frame.

In the near-infrared spectrum available for the eastern component of S we see three narrow emission lines corresponding to H β , [O III] $\lambda 4959$, and [O III] $\lambda 5007$, with unresolved rest-frame FWHM of $\lesssim 220 \text{ km s}^{-1}$ (corrected for the instrumental resolution). These features indicate a redshift for the emission-line gas in the system of $z = 3.0743 \pm 0.0001$, which we adopt as the systemic redshift for the galaxy.

Finally, the LRIS spectrum of G1 shows a strong continuum break around 6900 Å and several features that we identify as

Ca H and K, G band, and [O II] $\lambda 3727$ at $z = 0.7268 \pm 0.0007$. The [O II] $\lambda 3727$ line has an equivalent width of just 7.5 Å, indicating modest star formation activity. Thus, the likely lens appears to be an early-type spiral behind the cluster, and from the width of the G band and Ca H and K lines it indicates a central velocity dispersion of $\sim 230 \pm 30 \text{ km s}^{-1}$. In addition to this galaxy, we also serendipitously detect a further two galaxies that show [O II] 3727 at $z \sim 0.73$, indicating the presence of a structure at this redshift.

Turning to the broadband imaging, we compare the morphology of the arcs as seen in the NIRC K' -band image to the *HST* ACS F606W image. This shows no evidence for strong color variations within or between the two arcs, although the difference in resolution in the two bands and the presence of the lens makes this comparison difficult. We also see no evidence for a second lens in the system—with the position of G1 agreeing well between the optical and near-infrared images. We find that the arcs dominate the integrated light from the system from the g to K bands: measuring $K' = 18.9 \pm 0.1$ and $(R_{606} - K') \sim 1.7$ for the combined arcs and $K' = 19.7 \pm 0.1$ and $(R_{606} - K') \sim 2.8$ for G1. The color of G1 matches that of an early type spiral or S0 at $z = 0.73$, while the K' -band magnitude yields $M_K \sim -23.9 + 5 \log h$, indicating it is a $\sim L_K^*$ galaxy (consistent with its measured velocity dispersion and the Faber-Jackson relation).

3.2. Lensing Model

To interpret the properties of this system in more detail we have developed a lens model using the semilinear inversion method of Warren & Dye (2003). The model includes not only a mass component for G1 but also a significant external shear from the mass distribution in the foreground cluster at $z = 0.33$. The best-fit parameters for the galaxy-scale mass component are in good agreement with the observed light distribution and velocity dispersion of G1—the mass is centered on G1 with an ellipticity of $\epsilon = 0.31 \pm 0.01$ at a P.A. of $103^\circ \pm$

2° and a velocity dispersion $\sigma = 230 \pm 5 \text{ km s}^{-1}$. The cluster contributes an additional shear of $\gamma = 0.15$ along a direction tangential to the cluster center, which produces the offset in the centers of curvature of N and S. This lens model suggests a combined magnification for the arcs of 28 ± 3 . The model forms the arcs N/S from lensing of a single, extended background source with a scale size of $\sim 1 \text{ kpc}$. However, to reproduce the faint western extension of N we require a second background source, offset from the primary source by $\sim 0.3''$ ($\sim 2 \text{ kpc}$). The proximity of these two sources means that they likely represent two star-forming knots within a single galaxy. In this regard, we note that if the galaxy was not lensed, it would appear as a single elongated source even in deep ACS imaging. A more detailed description of the mass model for the lensing galaxy is given in S. Dye et al. (2007, in preparation).

3.3. Intrinsic Properties

Having determined the magnification of the system we can estimate the intrinsic luminosity of the background galaxy. First, we note that the characteristic apparent magnitude of $z \sim 3$ LBGs is $K^* = 22.52 \pm 0.25$ (Shapley et al. 2001). Hence, the K' -band magnitude of the arcs corresponds to an apparent luminosity of $28L_V^*$. Correcting for the lensing magnification of $\sim 28 \pm 3$, the arcs' intrinsic apparent magnitude translates to $K \sim 22.6 \pm 0.2$, consistent with L_V^* for the $z = 3$ LBG population (cf. Allam et al. 2007). Similarly, comparing the colors of the arcs, $(R_{606} - K') \sim 1.6$, with typical $z \sim 3$ LBGs, which have $(R - K) \sim 1.0 \pm 0.6$ (Shapley et al. 2001), we find that the arcs are slightly redder but are within the 1σ scatter for the population.

Finally, to estimate the star formation rate in the galaxy we use the R -band continuum magnitudes of the arcs to determine a rest-frame 1500 \AA luminosity of $L_{1500} \sim 4.6 \times 10^{30} \text{ ergs s}^{-1} \text{ Hz}^{-1}$, which translates into a star formation rate of $640 M_\odot \text{ yr}^{-1}$, adopting a Salpeter IMF with an upper mass cutoff of $100 M_\odot$ (Kennicutt

1998) and without any correction for reddening or magnification. Correcting for the estimated magnification and UV reddening, we derive an intrinsic star formation rate of $\sim 100 M_\odot \text{ yr}^{-1}$.

4. CONCLUSIONS

We report the discovery of an LBG at $z = 3.0743$ that is seen as a pair of arcs with an apparent magnitude of $r = 20.3$, equivalent to $28L_V^*$. This very bright apparent magnitude results from gravitational lensing by a galaxy at $z = 0.73$ and a cluster at $z = 0.33$, which provide a combined magnification of 28 ± 3 . Correcting for this magnification we show that LBG J213512.73–010143 (the cosmic eye) is a compact $\sim L_V^*$ LBG with moderate dust reddening, $E(B - V) \sim 0.4$, and a star formation rate of $\sim 100 M_\odot \text{ yr}^{-1}$. We illustrate the range of spectral features that can be identified in a modest S/N, moderate-resolution spectrum of the galaxy. The importance of this system is the opportunity it provides to obtain rest-frame UV, mid-infrared, and millimeter wave band observations of a typical $z \sim 3$ LBG at the resolution and S/N that will only become available for unlensed examples with the commissioning of ELTs, the *James Webb Space Telescope (JWST)*, or the Atacama Large Millimeter Array (ALMA). Such observations will provide unique information on the elemental abundances, star formation, gas mass, and dynamics of this young galaxy, facilitating a range of studies including the calibration of the various indicators proposed to trace the metallicity of gas in distant galaxies. This system can thus act as a pathfinder for the science that will be done with ELTs, *JWST*, and ALMA when they are completed.

We thank Max Pettini for help and useful discussions and an anonymous referee for constructive comments which improved this work. I. S. and G. P. S. acknowledge support from the Royal Society, and A. M. S. acknowledges support from PPARC.

REFERENCES

- Allam, S. S., Tucker, D. L., Lin, H., Diehl, H. T., Annis, J., Buckley-Greer, E., & Frieman, J. A. 2007, *ApJL*, submitted (astro-ph/0611138)
- Bentz, M. C., Osmer, P. S., & Weinberg, D. H. 2004, *ApJ*, 600, L19
- Calzetti, D., Armus, L., Bohlin, R. C., Kinney, A., Koornneef, J., & Storchi-Bergmann, T. 2000, *ApJ*, 533, 682
- de Mello, D. F., Leitherer, C., & Heckman, T. M. 2000, *ApJ*, 530, 251
- Ebeling, H., Edge, A. C., & Henry, J. P. 2001, *ApJ*, 553, 668
- Ellis, R. S., Santos, M. R., Kneib, J.-P., & Kuijken, K. 2001, *ApJ*, 560, L119
- Hook, I. M., ed. 2005, *The Science Case for the European Extremely Large Telescope: The Next Step in Mankind's Quest for the Universe* (Cambridge/Garching: OPTICON/ESO)
- Iverson, R. J., Smail, I., Bentz, M., Stevens, J. A., Menendez-Delmestre, K., Chapman, S. C., & Blain, A. W. 2005, *MNRAS*, 362, 535
- Kennicutt, R. C., Jr. 1998, *ARA&A*, 36, 189
- Kneib, J.-P., Ellis, R. S., Santos, M. R., & Richard, J. 2004a, *ApJ*, 607, 697
- Kneib, J.-P., van der Werf, P., Kraiberg Knudsen, K., Smail, I., Blain, A. W., Frayer, D., Barnard, V., & Ivison, R. 2004b, *MNRAS*, 349, 1211
- Leitherer, C., Leão, J. R. S., Heckman, T. M., Lennon, D. J., Pettini, M., & Robert, C. 2001, *ApJ*, 550, 724
- Leitherer, C., et al. 1999, *ApJS*, 123, 3
- Pettini, M., Rix, S. A., Steidel, C. C., Adelberger, K. L., Hunt, M. P., & Shapley, A. E. 2002, *ApJ*, 569, 742
- Pettini, M., Steidel, C. C., Adelberger, K. L., Dickinson, M., & Giavalisco, M. 2000, *ApJ*, 528, 96
- Santos, M. R., Ellis, R. S., Kneib, J.-P., Richard, J., & Kuijken, K. 2004, *ApJ*, 606, 683
- Shapley, A. E., Steidel, C. C., Adelberger, K. L., Dickinson, M., Giavalisco, M., & Pettini, M. 2001, *ApJ*, 562, 95
- Shapley, A. E., Steidel, C. C., Pettini, M., & Adelberger, K. L. 2003, *ApJ*, 588, 65
- Smail, I., Edge, A. C., & Ellis, R. S. 1998, *Publ. Astron. Soc. Australia*, 15, 267
- Smail, I., Ivison, R. J., Blain, A. W., & Kneib, J.-P. 2002, *MNRAS*, 331, 495
- Stern, D., et al. 2004, *ApJ*, 612, 690
- Warren, S., & Dye, S. 2003, *ApJ*, 590, 673